Geometric Predictors of Abdominal Aortic Aneurysm Maximum Wall Stress

Elver A. Pérez*[a], Luis R. Rojas-Solórzano[b], Ender Finol[c]

[a] Department of Energy Conversion and Transport. Universidad Simón Bolívar. Caracas, Venezuela
[b] Department. of Mechanical Engineering. Nazarbayev University. Astana, Rep. of Kazakhstan
[c] Department of Biomedical Engineering. University of Texas at San Antonio. San Antonio, Texas, USA
elveralejandro@gmail.com

Abdominal aortic aneurysm (AAA) is a dilation of the abdominal aorta (above 50 % of its original diameter), which can cause death upon rupturing. It usually grows asymptomatically leading to late clinical intervention. The medical criteria to indicate surgery are based on measuring the diameter and growth rate, but in many cases aneurysms fail at uncharacterized critical values. In search of a more efficient technique in predicting AAA failure, there is consensus on the importance of studying its geometric characteristics and estimation of the wall stress, but no fully successful correlation has been found between the two yet. This work examines the relationship between a parameterized geometry (18 input variables and 10 dependent indices) and 1 output variable: the maximum wall stress. Design of Experiments (DOE) techniques are used to generate 183 geometric configurations, for which Finite Element Analyses are performed using ANSYS[TM] state-of-the-art solver with a hyperelastic, isotropic and homogeneous arterial model for the wall, considering systolic internal pressure (steady state) and the restriction of longitudinal movement at the blood vessel end-sections. Due to the large number of independent parameters to consider, a preliminary Parameters Correlation analysis was performed to determine if a correlation between all input parameters and the maximum stress existed. The correlations between input parameters and the output variable were determined using the Spearman Rank correlation. Correlations with the maximum wall stress for: maximum diameter ($\rho = 0.46$), wall thickness ($\rho = -0.35$), d_c parameter ($\rho = 0.21$) and tortuosity ($\rho = 0.55$) were found. The response surface function between geometry and maximum wall stress was estimated by three models: Universal Kriging geostatistical regression (18 parameters), multiple linear regression (4 parameters) and multiple exponential regression (4 parameters). The models accounted for the stress variance by 99 %, 61 % and 66 %, respectively, with average percentage errors of 0.12 %, 16 % and 17 %, respectively. The solution spaces obtained from this study might provide physicians with a better estimation of the AAA rupture potential and thus, facilitate safer and anticipated treatments of the condition.

1. Introduction

Abdominal aortic aneurysm (AAA) is the expansion of the abdominal aorta (> 50 % of its original diameter), which can rupture if left untreated, an event that carries a high mortality rate (Crawford et al., 2003). The true incidence of ruptured abdominal aortic aneurysms varies between 2 and 15 admissions per 100,000 patients depending on the population (Somolock and Lyden, 2014). The medical criterion for the prevention of rupture is based on measuring the diameter (Shimazaki and Ueda, 2014) and growth rate (Hinchliffe et al., 2003). Nevertheless, there have been numerous cases of AAA rupture that occur at a maximum diameter and/or growth rate different from the critical values (Crawford et al., 2003). Therefore, interest has emerged in the search for a better criterion in predicting the failure of the arterial wall. The multitude of factors that affect the behaviour of the aneurysm makes more difficult to establish a general criterion for an adequate description of the complex pathogenesis of the disease, suggesting the use of specific criteria for each patient. Fillinger et al., (2003) concluded that the estimation of stress on the arterial wall can help determine the risk of rupture with greater accuracy than considering only the diameter. Advances in clinical imaging (ex: CT, MRI) have enabled the study of patient-specific geometries and verification of the existence of a relationship between

physical parameters associated with the asymmetry (Doyle et al., 2009), torsion, tortuosity, curvature (Georgakarakos et al., 2009), and wall thickness (Shang et al., 2013) with the maximum stress on the arterial wall. Martufi et al., (2009) demonstrated the convenience of geometric relationships and suggested proposals for consideration of the above in estimating the risk of rupture. In recent years, many advances in new models and improved boundary conditions have been made, but a correlation between physical characteristics and the maximum stress in the AAA wall has not been found yet. Thus, this investigation addresses for the first time, based on Design of Experiments (DOE) techniques, the computational analysis of a broad range of AAA CAD-generated geometries, using 18 input parameters, to identify which geometric characteristics are closely related with arterial wall stress. In addition, with the use of computational and statistics tools, we determine relationship between these characteristics and the maximum wall stress.

2. Methodology

A set of AAA CAD geometries was generated based on the DOE for all the input parameters. The numerical simulation for each of these case studies was performed using ANSYS-Structural Mechanics[TM], based on the solution of the system of three-dimensional equations of displacement and stress equilibrium discretized using the Finite Element Method.

2.1 Arterial wall model
The middle aorta can be considered a homogeneous and incompressible medium (Vande Geest et al., 2008). Considering that tissue anisotropy is not present in all cases, a quasi-incompressible isotropic hyperelastic model based on a Mooney-Rivlin equation of 5 material constants – Eq(1), was obtained through a process of linear regression to fit the stress-strain experimental data reported by Raghavan and Vorp (2000):

$$W = C_{10}(\bar{I}_1 - 3) + C_{01}(\bar{I}_2 - 3) + C_{20}(\bar{I}_1 - 3)^2 + C_{11}(\bar{I}_1 - 3)(\bar{I}_2 - 3) + C_{02}(\bar{I}_2 - 3)^2 + \frac{1}{d}(J - 1)^2 \tag{1}$$

C_{10} = 1.324 x 10^6 Pa; C_{01} = -1.231 x 10^6 Pa; C_{20} = -4.499 x 10^7 Pa;
C_{11} = 4.475 x 10^7 Pa; C_{02} = 1.413 x 10^7 Pa; D_1 = 0.0 Pa^{-1}

$\bar{I}_1$ and $\bar{I}_2$ are the first and second right Cauchy-Green strain tensor deviatoric invariants, and J is the volumetric ratio. This model is a truncation (N = 2) of the polynomial form of the potential function for quasi-incompressible materials (Celigueta, 2009).

2.2 Geometric model, parameters and indices
The AAA were numerically-generated by varying a set of geometric parameters at five (5) cross-sections illustrated in Figure 1. Disregarding the presence of thrombus to simplify the geometry, the number of independent parameters that can be used to generate an AAA is 18. In addition, ten (10) dependent indices based on the 25 indices proposed by Martufi et al., (2009) were used: L, d_c, H_b, V, DHr, DDr, Hr, Bl, β and T. L is the sum of lengths of straight lines connecting the five cross-section centroids; d_c is the perpendicular distance from the centroid at the maximum diameter to the vertical axis path from the centroid at section I; H_b is the vertical distance between D_{neck1} and D_{max} centroid cuts; V is the aneurysm volume; DHr, DDr, Hr, Bl, β and T are 2-dimensional shape indices and are calculated as indicated in Table 1. β is a degree of AAA sac asymmetry and T the tortuosity of the aneurismal aorta.
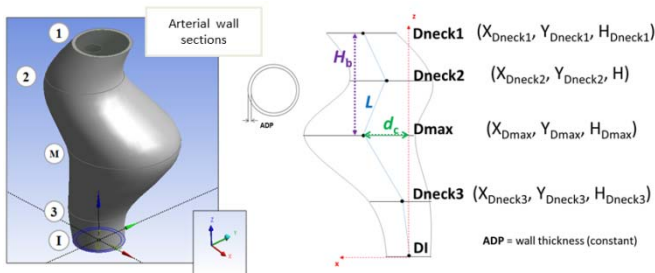

Figure 1: Visualization of sections in AAA and the 18 independent parameters.

Table 1: Two-dimensional shape indices

DHr	DDr	Hr	Bl	B	T
$\dfrac{D_{max}}{H}$	$\dfrac{D_{max}}{D_{neck1}}$	$\dfrac{H}{H_{Dneck1} - H}$	$\dfrac{H_b}{H}$	$\dfrac{d_c}{D_{max}}$	$\dfrac{L}{\sqrt{(H_{Dneck1})^2 + (X_{Dneck1})^2 + (Y_{Dneck1})^2}}$

2.3 Boundary conditions, domain and mesh density
A steady state analysis is proposed, subjecting the endoluminal surface of the aneurysm to 120 mmHg (1.6 N/cm^2) to simulate peak systolic conditions when maximum wall stress is achieved (Raghavan and Vorp, 2000). The displacement in the longitudinal direction at the end of the model is restricted. The verification of the domain extension and mesh density are performed in the CAD model using a simple geometry. The longitudinal extension of the axial domain was established to ensure circumferential displacement at the ends of AAA without change (< 1 %) in global maximum principal stress σ_{pmaxg}, strain ε_{pmaxg} and average strain in the inner wall of section I. The mesh was generated using tetrahedrons of 10 nodes - SOLID 187 (Ansys, Inc., 2009). Its density was selected studying the error (L$_2$-norm), calculated as described by Prakash and Ethier (2001), of the maximum principal stress σ_{pmax} along an internal wall line from section I to section M. The error of the L$_2$-norm was less than 1 x 10^{-3} for a mesh with density of 2,620 elements/cm^3 (114,000 elements approximately), compared to a mesh with a density of 566 elements/cm^3.

2.4 Design of experiments (DOE)
The experimental design is a technique used to determine the location of sampling points so that the input parameter space is scanned in the most efficient manner. Optimal Space-Filling (OSF), is one scheme in DOE that creates an experimental design set by using one of several available algorithms to fill the discrete space of design. In this study, the OSF is based on the maximum-minimum distance (Maximin) algorithm, developed by Johnson, Moore and Ylvisaker (1990). Case studies were selected from the space limits given in Table 2 and thus, 190 design points were created by the OSF sampling.

Table 2: Limits of variation of independent parameters

Parameters	Min (cm)	Max (cm)	Parameters	Min (cm)	Max (cm)	Parameters	Min (cm)	Max (cm)
D$_I$, D$_{neck1}$	2.0	3.0	ADP	0.15	0.25	D$_{neck2}$, D$_{neck3}$	2.0	4.0
H$_{Dneck1}$	11.5	12.5	H	9.0	11.0	H$_{Dneck3}$	1.0	3.0
D$_{max}$, H$_{Dmax}$	4.0	8.0	X$_{Dneck1}$, Y$_{Dneck1}$	-1.0	1.0	X$_{Dmax}$, Y$_{Dmax}$	-2.0	2.0
X$_{Dneck2}$, Y$_{Dneck2}$	-2.0	2.0	X$_{Dneck3}$, Y$_{Dneck3}$	-2.0	2.0			

2.5 Correlation matrix and response surface
Following the results of the numerical simulations, a probabilistic sensitivity analysis was performed to evaluate the correlation between variables calculating the Spearman correlation coefficient ρ (Sheskin, 2004) for each pair of parameters, facilitating the selection of geometric indices of greater relevance correlated with wall stress. An adjustment of the dependent parameters was performed as a function of the input variables through regression analysis techniques. A Response Surface (RS) was obtained for the output parameter using, in a first stage, a Universal Kriging with all 18 input parameters, while in a second stage (using least squares linear and exponential regressions), only the well-correlated variables were chosen for the fitting.

Universal Kriging assumes that there is a trend that can be modeled by a deterministic polynomial function, which combines with a random function to predict the values at points within the feasible space of input variables (ArcGIS Resource Center, 2011). The unknown output function y(x) is the result of the sum of a polynomial form of f(x) that "globally" approximates the design space and Z(x), which is the realization of a Gaussian random process normally distributed with a zero mean, variance σ^2 and nonzero covariance that creates "localized" deviations so that the Kriging model interpolates the N sampling points (Ansys Inc., 2009).

The multiple linear regression model with q variables corresponds to (Pértega and Pita, 2000):

$$\sigma_i = \alpha_0 + \alpha_1 x_{i1} + \alpha_2 x_{i2} + \cdots + \alpha_q x_{iq} + \varepsilon_i \qquad i = 1,2 \dots N \tag{2}$$

The α_j coefficients are estimated following the least squares criterion:

$$\alpha = (X^T X)^{-1} X^T \sigma \tag{3}$$

The multiple exponential regression model with q variables responds to the Eq(4):

$$\sigma_i = \gamma_0 (\gamma_1^{x_{i1}} \gamma_2^{x_{i2}} \times \dots \times \gamma_q^{x_{iq}}) \tag{4}$$

By linearizing Eq(4), it yields an equation analogous to Eq(2):

$$\ln\sigma_i = \ln\gamma_0 + x_{i1}\ln\gamma_1 + x_{i2}\ln\gamma_2 + \cdots + x_{iq}\ln\gamma_q + \varepsilon \tag{5}$$

where the least squares estimators are obtained from Eq(6), analogous to Eq(3):

$$\ln\gamma = (X^T X)^{-1} X^T \ln\sigma \tag{6}$$

3. Results

3.1 Global Maximum Principal Stress

Computer simulations of the 190 case studies were generated according to the DOE matrix and were successfully completed in approximately 1300 cpu-hours (Intel Core i5 CPU Processor, 4.00 GB of RAM). Figure 2 shows the geometry for the first eight designs. Geometries #113 and #172 presented the lowest (0.22 MPa) and the highest (1.18 MPa) σ_{pmaxg}, respectively, as can be seen in Figure 3. The latter geometry not only exhibits a maximum diameter (7.88 cm) larger than geometry #113 (5.13 cm), but also has a thinner wall (0.18 cm vs. 0.24 cm), is more asymmetric (β = 0.24 vs. β = 0.16) and more tortuous (T = 1.33 vs. T = 1.03). Geometry #113 had the lowest σ_{pmaxg} from the 190 case studies, even when its maximum diameter was not the lowest. The geometry with the lowest maximum diameter (geometry #50, D_{max} = 4.01 cm) had a higher maximum wall stress than 66 other AAA. This implies that using only maximum diameter as a surrogate for peak wall stress is insufficient. In the present study the average maximum wall stress was 0.56 MPa (0.22 - 1.18 MPa).
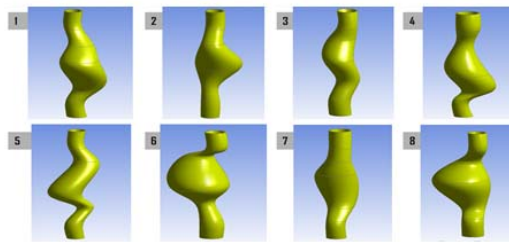

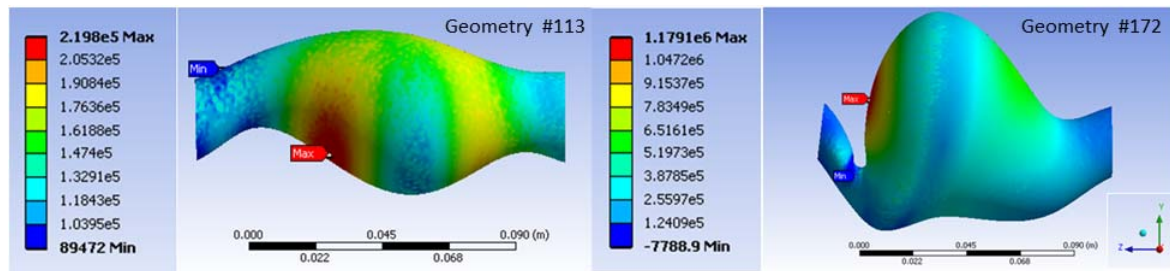Figure 2: Geometry for the first eight designs.

Figure 3: Maximum principal stress distribution [Pa] in geometries #113 and #172.

3.2 Correlation matrix

According to the ratio-range scale of Martinez et al. (2009), σ_{pmaxg} had a low correlation with d_c (ρ = 0.21), a weak correlation with D_{max} (ρ = 0.46), ADP (ρ = - 0.35), DHr (ρ = 0.43) and DDr (ρ = 0.41), and a moderate correlation with L (ρ = 0.52) and T (ρ = 0.55). The most important parameters in the study were D_{max}, ADP, L, d_c, DHr, DDr and T; choosing non-collinear parameters, D_{max}, the wall thickness ADP, the Euclidean distance d_c, and tortuosity T were chosen for the final Response Surface (RS).

3.3 Response surface

The universal Kriging technique generated a solution space of 18 + 1 dimensions (18 input parameters, and 1 output parameter) to estimate σ_{pmaxg}. Taking configurations #113 and #172 as the limiting cases, Figure 4(a) shows σ_{pmaxg} as a function of wall thickness for both AAA, showing the nearly linear relationship between wall stress and thickness with a maximum wall stress up to 20 % higher for a wall thickness of 1.5 mm compared to 2.5 mm. Figure 4(b) depicts the nonlinear increase in wall stress when the maximum diameter is larger than 5 cm. Given the fitted response surface, σ_{pmaxg} can be analyzed as a function of select input parameters while leaving the remaining parameters constant. Such is the case of Figures 5(a) and (b), where the maximum diameter and D_{neck1} were chosen, illustrating the variation of the output parameter in geometries #113 and #172. For AAA #113, the stress is nearly independent of D_{neck1}, while for AAA #172 there is an evident dependency of stress on this parameter. These results confirm the influence of the global geometry in the response of AAA wall stress to intraluminal pressure. The response surface (RS) allows estimation of the maximum wall stress without the need to carry out the respective numerical analysis. The RS may provide both the initial prognosis of an AAA according to its geometric characteristics and also exploring possible

follow-up scenarios by varying any of the independent parameters. Figures 5(c) and (d) illustrate the RS for the wall stress vs. D_{max} and wall thickness (the most influential parameters) for AAA #113 and #172.
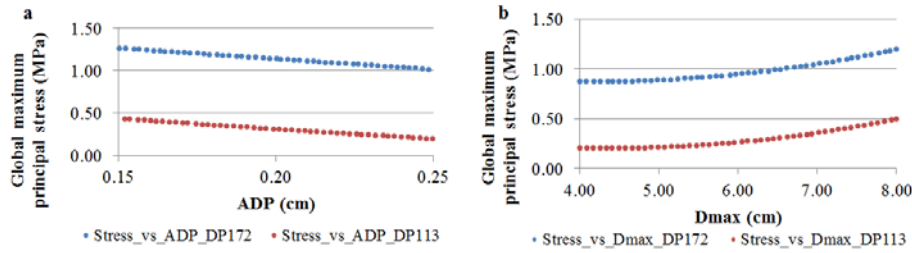

Figure 4: a, Global maximum principal stress as a function of wall thickness for #113 and #172; b, Global maximum principal stress as a function of maximum diameter for #113 and #172.
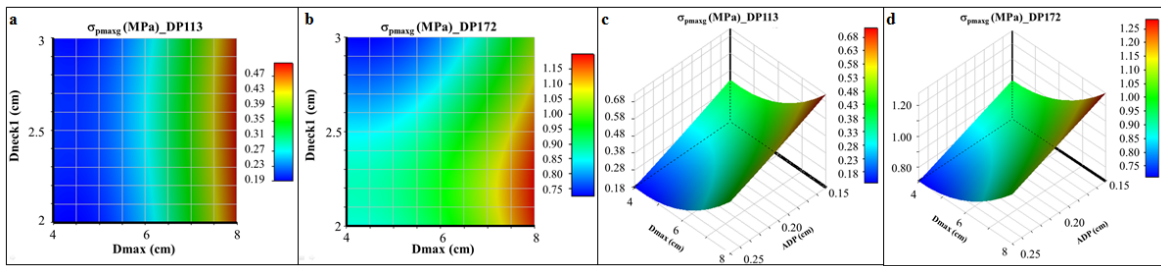

Figure 5: a, b Contours of σ_{pmaxg} vs. D_{max} and D_{neck1} in geometries #113 and #172; c, d Contours of σ_{pmaxg} vs. D_{max} and ADP in geometries #113 and #172.

After reducing the initial space to the few parameters that resulted in high correlation factors, the fitted Eq(2) leads to the following expression:

$$\sigma_i = \alpha_0 + \alpha_1 D_{max} + \alpha_2 ADP + \alpha_3 T + \alpha_4 d_c \tag{7}$$

The least-square fitted coefficients according to Eq(3) are:
α_0 = -1.0081 x 10^6; α_1 = 8.1334 x 10^4; α_2 = -2.1806 x 10^6; α_3 = 1.2710 x 10^6; α_4 = -8.1175 x 10^3
For the same limited set of parameters, Eq(4) leads to the following multiple exponential regression:

$$\sigma_i = \gamma_0 (\gamma_1^{D_{max}} \gamma_2^{ADP} \gamma_3^{T} \gamma_4^{d_c}) \tag{8}$$

γ_0 = 3.1944 x 10^4; γ_1 = 1.1627; γ_2 =0.0176; γ_3 =9.5816; γ_4 =0.9925
The coefficient of determination R^2 and the statistical significance through global contrast regression F (Sheskin, 2004) were calculated to measure the goodness of fit of the two correlations expressed by Eq(7) and Eq(8). The values obtained (R^2 = 0.61 and R^2 = 0.66, respectively) indicate that the models explain 61 % and 66 % of the variability of the maximum principal stress. These results, the statistical significance (F = 69.8 and F = 88.1, respectively) and the probability p of occurrence of the regression F (p << 0.01 for both correlations) indicate that much of the variance of σ_{pmaxg} is explained by the fitted models.

4. Conclusions

Correlations between the geometry and maximum stress of the arterial wall in AAAs were developed based on numerical stress analyses of CAD-generated geometries using Design of Experiments (DOE) to build surrogate or response surface models. The results of calculating the maximum wall stress in 190 AAA geometries allowed the development of three correlations: a regression based on the Universal Kriging geostatistical model, a multiple linear regression based on four independent parameters (D_{max}, ADP, d_c, and T) and a multiple exponential regression also based on these four parameters. These correlations have average percentage errors of 0.12 %, 17 % and 16 %, respectively. Calculating wall stress by means of finite element modeling is a relatively complex process to implement clinically, so the idea of being able to estimate wall stress based on geometric correlations has high translational value. In the present work we found three models that accounted for more than 60 % of the wall stress variance in the 190 idealized geometries. These models may ultimately guide the initial diagnosis of AAA in terms of their geometry, allowing the use of indices

other than the maximum diameter to predict their risk of rupture. The response surfaces (RS) obtained allowed the estimation of maximum wall stress for any combination of input variables under the physically constrained ranges without the need of a new finite element analysis simulation. We demonstrated that maximum wall stress can be predicted relatively accurately by measuring maximum diameter, wall thickness, the Euclidean distance between centroids at the maximum and inlet cross-sections, and the tortuosity of the AAA, all of which can be characterized with modern and inexpensive clinical imaging technology. The development of these new correlations is not intended to replace a patient-specific stress analysis, but rather provide simple tools vascular surgeons or interventional radiologists can use to make a first assessment of the disease severity in an individual. These tools are based on the assessment of more than just the clinically relevant maximum diameter and do not require a lengthy process of image segmentation, generation of the patient-specific geometry, or finite element modeling to estimate the maximum wall stress.

Reference

ANSYS Inc., 2009, Structural Analysis Guide Release 12.0, ANSYS Inc, Canonsburg, United States.

ArGIS Resource Center, 2011, Cómo funciona Kriging. <http://help.arcgis.com/es/arcgisdesktop/10.0/help/index.html#//009z00000076000000> accessed 28.05.12

Celigüeta, J. T., 2009, Análisis de estructuras con no linealidad geométrica, 2nd Ed., Unicopia C. B., Gipuzcoa, España.

Crawford, C. M., Hurtge-Grace, K., Talarico, E., Marley, J., 2003, Abdominal aortic aneurysm: An illustrated narrative review, Journal of Manipulative and Physiological Therapeutics, 26 (3), 184-195.

Doyle, B. J., Callanan, A., Burke, P. E., Grace, P. A., Walsh, M. T., Vorp, D. A., McGloughlin, T. M., 2009, Vessel asymmetry as an additional diagnostic tool in the assessment of abdominal aortic aneurysms, Journal of Vascular Surgery, 49 (2), 443-454.

Fillinger, M. F., Marra, S. P., Raghavan, M. L., Kennedy, F. E., 2003, Prediction of rupture risk in abdominal aortic aneurysm during observation: Wall stress versus diameter, Journal of Vascular Surgery, 37 (4), 724-732.

Georgakarakos, E., Ioannou, C. V., Kamarianakis, Y., Papaharilaou, Y., Kostas, T., Manousaki, E., Katsamouris, A. N., 2009, The Role of Geometric Parameters in the Prediction of Abdominal Aortic Aneurysm Wall Stress, European Journal of Vascular & Endovascular Surgery, 39, 42-48.

Hinchliffe, R. J., Alric, P., Rose, D., Owen, V., Davidson, I. R., Armon, M. P., Hopkinson, B. R., 2003, Comparison of morphologic features of intact and ruptured aneurysms of infrarenal abdominal aorta, Journal of Vascular Surgery, 38 (1), 88-92.

Johnson, M. E., Moore L. M., Ylvisaker D., 1990, Minimax and maximin distance designs, Journal of Statistical Planning and Inference, 26, 131-148.

Martínez, R. M., Tuya, L. C., Martínez, M., Pérez, A., Cánovas, A. M., 2009, El coeficiente de correlación de los rangos de Spearman caracterización, Rev haban cienc méd [online] 8(2), <http://scielo.sld.cu/scielo.php?script=sci_arttext&pid=S1729-519X2009000200017&lng=es> accessed 15.05.12

Martufi, G., Di Martino, E. S., Amon, C. H., Muluk, S. C., Finol, E. A., 2009, Three-Dimensional Geometrical Characterization of Abdominal Aortic Aneurysms: Image-Based Wall Thickness Distribution, Journal of Biomechanical Engineering, 131(6), 061015.

Pértega, S., Pita, S., 2000, Técnicas de regresión: Regresión Lineal Múltiple, Cad. Aten Primaria, 7, 173-6.

Prakash, S., Ethier, C. R., 2001, Requirements for mesh resolution in 3D computational hemodynamics. Journal of biomechanical engineering, 123(2), 134-144.

Raghavan, M. L., Vorp, D. A., 2000, Toward a biomechanical tool to evaluate rupture potential of abdominal aortic aneurysm: identification of a finite strain constitutive model and evaluation of its applicability, Journal of Biomechanics, 33, 475-482.

Shang, E. K., Nathan, D. P., Woo, E. Y., Fairman, R. M., Wang, G. J., Gorman, R. C., Gorman J. H., Jackson B. M., 2013, Local wall thickness in finite element models improves prediction of abdominal aortic aneurysm growth, Journal of Vascular Surgery, DOI: 10.1016/j.jvs.2013.08.032

Sheskin, D. J., 2004, Handbook of Parametric and Nonparametric Statistical Procedures, 3th Ed., United States, Chapman & Hal/CRC.

Shimazaki, Y., Ueda, H., 2014, Abdominal Aortic Aneurysm, Interdisciplinary Concepts in Cardiovascular Health, 161-179.

Smolock, C. J., Lyden, S.P., 2014, Abdominal Aortic Aneurysm, Cleveland Clinic Manual of Vascular Surgery, 3-12.

Vande Geest, J. P., Schmidt, D. E., Sacks, M. S., Vorp, D. A., 2008, The Effects of Anisotropy on the Stress Analyses of Patient-Specific Abdominal Aortic Aneurysms, Annals of Biomedical Engineering, 36 (6), 921-932.